EFFECT OF EXHAUST GAS RECIRCULATION ON DIESEL COMBUSTION

Aleš Hribernik, Niko Samec
University of Maribor, Faculty of Mechanical Engineering
Smetanova 17, SI-2000 Maribor, Slovenia
Telephone: +386 2 220 7731, Fax: +386 2 220 7990
e-mail: ales.hribernik@uni-mb.si

Abstract

Exhaust gas recirculation (EGR) is effective for the reduction of NOx emission from internal combustion engines. Although there has been extensive experimental research on emission formation by the application of EGR, little has been devoted to the diesel combustion process. An attempt was made to study experimentally the combustion process at different EGR rates and engine loads. A heavy duty turbocharged diesel engine was used for the tests and a low pressure EGR concept was applied. Different EGR rates were obtained simply by the position of EGR control valve. Exhaust gases were analysed for emissions of NOx, CO, HC and soot. In-cylinder pressure traces were measured and analysed. A one-zone combustion model was used to compute the rate of heat release from the experimental results. Several combustion parameters such as ignition delay, duration of pre-mixed and diffusion flame, combustion duration, etc., were determined and carefully studied, and basic correlation is presented and discussed in this paper.

1. Introduction

Exhaust gas recirculation (EGR) is effective for the reduction of NOx emission from internal combustion engines under all load conditions. High load NOx reduction in diesel engines is especially important because approximately 60 % of the NOx produced during U.S. emission tests and approximately 70 % of the NOx produced during European emission tests is produced at high load [1]. Researchers observed 30 % to 75 % reductions in NOx when using 5 % to 25 % EGR rates [1, 2].

Several explanations have been proposed for the reduction in NOx emissions using EGR. These explanations focus on EGR's reduction of the peak temperature within the post-flame zone [3]. Reduction of temperature in the post-flame zone where the formation of thermal NO takes place is caused by a combination of reduced oxygen concentration within the cylinder and the increased heat capacity of the in-cylinder gases. Reduced oxygen concentration reduces the temperature in the post-flame zone by the fact that, for the same amount of fuel which is to be burned, the same amount of oxygen is necessary. Thus a larger mass of gases has to be drawn through the flame front when the oxygen concentration is low, and the temperature increase in the post-flame zone is reduced since the same heat is released by the combustion. It is postulated [4] for diesel combustion that the reduced oxygen concentration contributes 90 % to the reduction of post-flame zone temperature, and that the contribution made by the increased heat capacity of the in-cylinder gases is just 10 %.

The effects of EGR on diesel combustion have already been studied by Uchida [2]. It was found that ignition delay rose with EGR rate, however, an increase in the initial heat release rate was not observed. Mitchell [5], however, reported substantial increase in premixed burn fraction with increasing dilution of the intake mixture by nitrogen (simulated EGR), while Zhao [6] observed substantial reduction in ignition delay by the unchanged ratios of heats released by premixed and diffusion combustion with increasing dilution of intake mixture by carbon dioxide. This shows that there are important differences between different EGR approaches, testing conditions and engine types, and that simple generalisation of the results may be misleading. A study of individual engines is, therefore, necessary to acquire better insight into the effects of EGR on its combustion process.

2. Experimental system

A heavy duty 4-cylinder 7,2 litre turbocharged diesel engine was investigated. The characteristics of this engine are summarised in Table 1.

Table 1. Test engine specifications

Engine	Turbo Diesel, 4-stroke, DI
Fueling	BOSCH In-Line Pump
Number of Cylinders	4
Bore x Stroke	125 mm x 145 mm
Total Displacement	7117 cm^3
Compression Ratio	15.8
Turbocharger	Holset H1E8264AD/GA26*11

Low-pressure EGR concept (Fig. 1) was applied. A passage was provided for the exhaust gases from below the turbine to pass to the fresh air side of the engine. The positive pressure difference across the appropriate EGR valve made EGR possible over a wide range of engine operating conditions. A diesel particulate filter was used in order to avoid increased wear on the compressor blades, and charge air cooler contamination. Recirculated gas was externally cooled by water to gas heat exchanger, and the gas temperature was maintained at 303 K by a controlled flow of cooling water. The engine on the test bed was fully instrumented. A computer-aided data acquisition system was applied to acquire high speed engine data (in-cylinder pressure, injection needle lift and injection pressure) versus crank angle. An additional data acquisition system was used for low speed engine data logging. Exhaust gas emissions were measured simultaneously. The actual EGR rate was predicted from the reduced mass flow rate of fresh inflow air as:

$$EGR = \frac{\dot{m}^*_{0,air} - \dot{m}_{air}}{\dot{m}^*_{0,air}} \cdot 100\% \cong \frac{\dot{m}_{EGR}}{\dot{m}_{air} + \dot{m}_{EGR}} \cdot 100\% \qquad (1)$$

where:

$\dot{m}^*_{0,air}$ - fresh air mass flow with closed EGR valve, corrected for the actual pressure and temperature ahead of the cylinder,

$\dot{m}_{air}$ - fresh air mass flow with opened EGR valve,

$\dot{m}_{EGR}$ - recirculated exhaust gas mass flow.

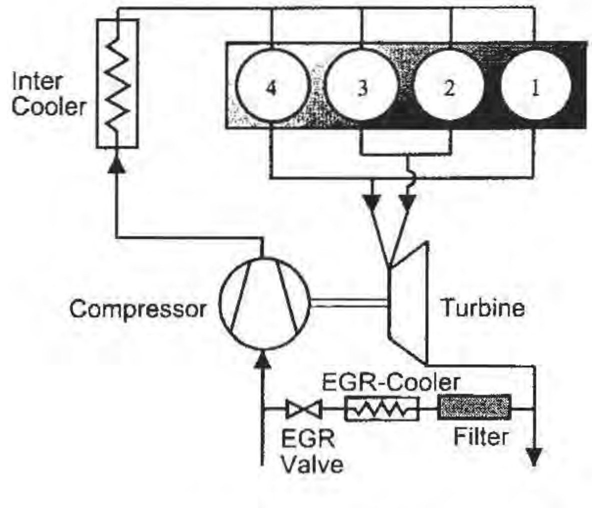

Fig. 1. Test engine setup

3. Results and discussion

Measurements were performed at three different engine speeds (1200, 1600 and 2000 rpm) and two engine loads (p_e= 5 bar and p_e= 9 bar) with EGR rates varying between 0 and 21 %.

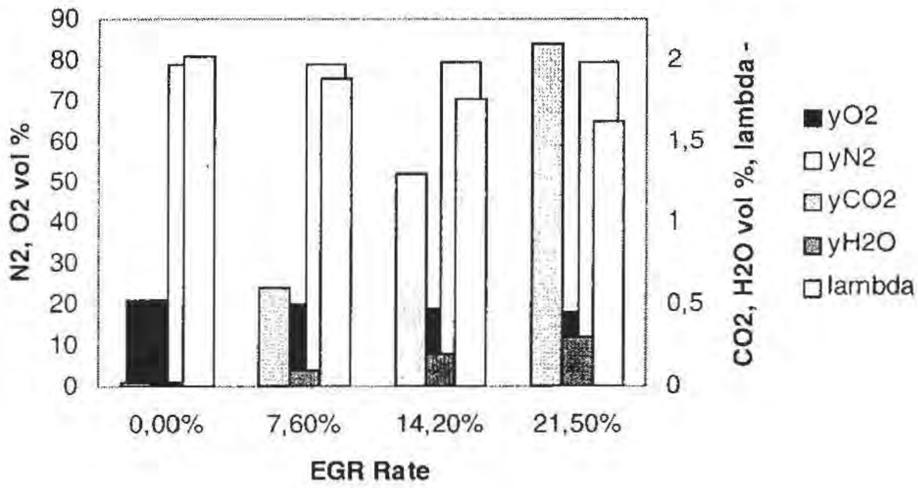

Fig. 2. Predicted intake gas mixture composition and measured equivalence air ratio λ at 1600 rpm and p_e= 9 bar

3. 1. Effect of EGR on the composition of intake gas mixture

Temperature of intake gas mixture was held constant by EGR cooler and just a slight increase in boost pressure with increasing EGR rate was observed at all analysed engine operation regimes. Thus it may be assumed that the gas exchange process and therefore total gas flow were not effected much by EGR. However, the overall equivalence air-fuel ratio λ decreased significantly with increasing EGR rate as shown in Fig. 2. Some of the oxygen was replaced by carbon dioxide, water vapour, nitrogen and other gaseous components of exhaust gases. If the latter are neglected the concentration of main components in the intake mixture can be predicted easily. Fig. 2 shows the measured overall equivalence ratio λ and predicted concentration of oxygen, carbon dioxide, water vapour and nitrogen. Most of the water vapour condensed within the EGR cooler, therefore, its concentration was lower and the increase in heat capacity of the intake mixture was mainly caused by carbon dioxide. However, the overall increase was small, no higher than 1 % [7]. The main influence on NOx reduction had, therefore, the reduction of oxygen concentration which was as high as 14 % for 21 % EGR rate.

3. 2. Effect of EGR on the exhaust gas emissions

A typical effect of EGR on the exhaust gas emissions of investigated engine is shown in Table 2. NOx was already reduced drastically with 7,6 % EGR. It was reduced by more than 65 % with 21,5 % EGR. Almost no EGR effect on the emissions of the unburned hydrocarbons (HC) was observed. However, the emissions of carbon monoxide and particulates tripled with 21,5 % EGR. In this particular case it can be seen that 14,2 % EGR was optimal, NOx emissions were reduced by more than 50 %, while CO and particulate emissions were still satisfactory.

Table 2. Influence of EGR on engine emissions at 1600 rpm and p_e= 9 bar (in comparison with 0 % EGR emissions in %)

EGR rate	λ (-)	CO	O2	HC	NOx	Soot
0 %	2,019	100	100	100	100	100
7,6 %	1,884	141	95	121	60	250
14,2 %	1,767	192	86	119	44	250
21,5 %	1,630	323	74	119	34	450

3. 3. Effect of EGR on the combustion

Fig. 3 shows four in-cylinder pressure traces measured under constant engine-operational conditions using different EGR rates. Two pronounced slope changes are observed in all four pressure traces. The first indicates the start of combustion, and the second, the end of combustion of the premixed reactants.

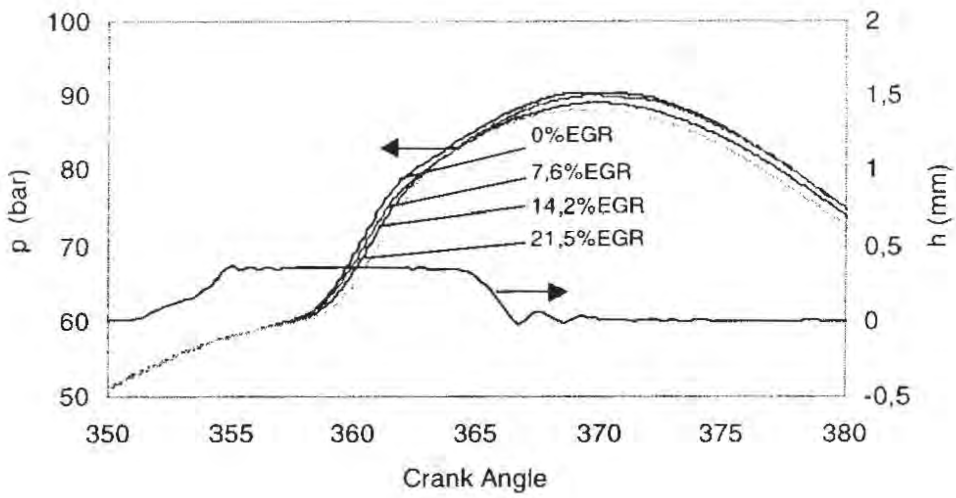

Fig. 3. Pressure traces with different EGR rates and injector needle lift trace at 1600 rpm and p_e= 9 bar

3.3.1. Ignition delay

Pressure traces were used to determine the ignition delay by subtracting the timing at the start of injection t_{inj} from the timing at the start of combustion t_{ign}. The start of injection t_{inj} was determined from the injector needle lift diagram (Fig. 3) and the start of combustion t_{ign} by analysing the derivative of the in-cylinder pressure curve. The ignition delay period is controlled by several physical and chemical factors and, therefore, is divided into physical and chemical ignition delays [8]. The physical delay consists primarily of the time needed to form an air-fuel mixture, whilst the chemical delay is due generally to the preflame oxidation reactions. Haywood [3] proposed a simple model for prediction of ignition delay. The equation that is correlated with cylinder pressure p_{cyl} and temperature T_{cyl} is used to calculate ignition delay ID as

$$ID = 3{,}45 \cdot \left(\frac{p_{cyl}}{101300} \right)^{-1.02} \cdot \exp\left(\frac{2100}{T_{cyl}} \right) \tag{2}$$

Since the in-cylinder conditions are not constant during ignition delay, equation (2) is integrated in time starting from fuel injection

$$\int_{t_{inj}}^{t} \frac{dt}{ID}$$

until it equals 1, when one can write

$$\int_{t_{inj}}^{t_{ign}} \frac{dt}{ID} = 1, \tag{3}$$

and the ignition delay

$$ID = t_{ign} - t_{inj},$$

averaged over changing in-cylinder conditions can be obtained. It is obvious that equation (2) originates from Arhenious law, and thus actually represents a chemical ignition delay.

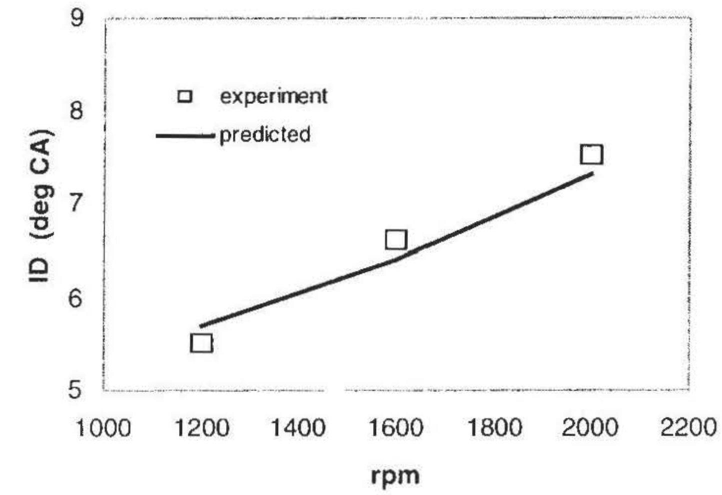

Fig. 4. Experimentally obtained and predicted ignition delay with 0 % EGR (p_e= 9 bar)

Adopting the constants in the equation (2) for the particular engine, the model can be successfully applied for ignition delay prediction as shown in Fig. 4. Thus it may be expected, that the model could be successfully used with different EGR rates as well. As seen from Fig. 5, however, the predictions were accurate only without EGR, and the characteristic ignition delay increase with increasing EGR rate (Fig. 5) was not predicted well, although the actual composition of intake gas mixture (reduced O_2 and increased CO_2, N_2 and H_2O concentration) was considered in computations. Therefore it may be assumed that there is a significant influence of the reduced O_2 in the intake mixture on the ignition delay, and that the reduced O_2 slowed down the pre-oxidation processes and therefore increased ignition delay.

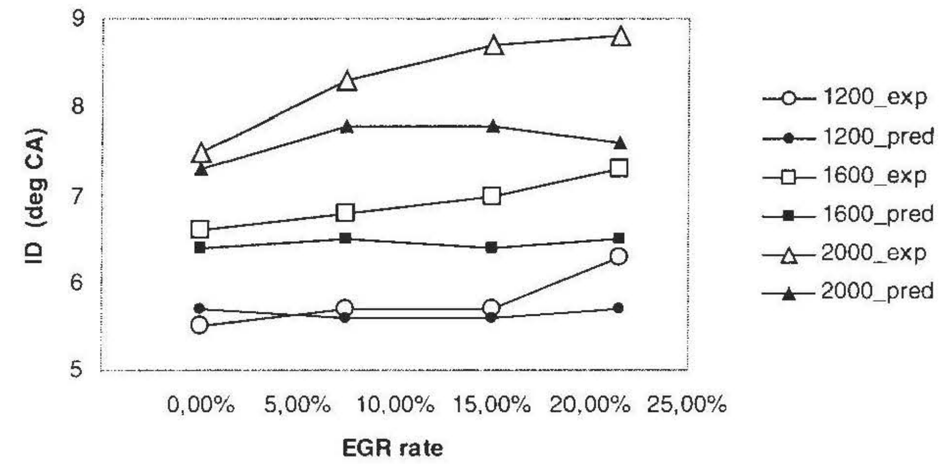

Fig. 5. Experimental and predicted ignition delay with different EGR rates (p_e= 9 bar)

In order to obtain better accuracy of the model with different EGR rates, the equation (2) was supplemented by simple part representing the reduction of O_2 in the intake mixture

$$R_{O_2,mix} = \frac{y_{O_2,mix}}{y_{O_2,air}} = \frac{y_{O_2,mix}}{0{,}21},$$

and the corrected equation writes

$$ID = 3{,}45 \cdot \left(\frac{p_{cyl}}{101300}\right)^{-1{,}02} \cdot \exp\left(\frac{2100}{T_{cyl}}\right) \cdot R_{O_2,mix}^{-A} \tag{4}$$

Optimising equation (4) for A gave a very good results over a wide range of engine operating regimes and EGR rates (Fig. 6).

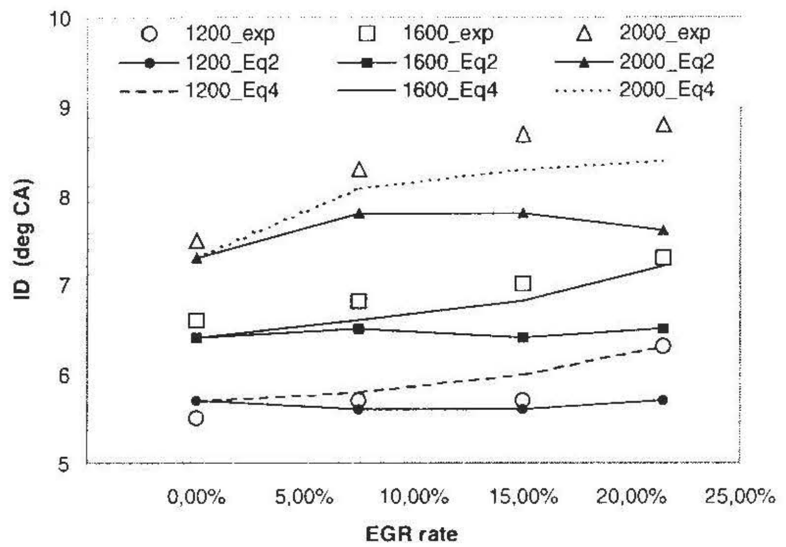

Fig. 6. Experimental and predicted ignition delay (original Eq2 and corrected Eq4 model) with different EGR rates (p_e= 9 bar)

3.3.2. Rate of heat release curves

Measured pressure traces were used for the determination of combustion heat release rates. Cylinder mass and energy conservation equations were numerically integrated using a personal computer. The results are shown in Fig. 7. Similar RHR (Rate of Heat Release)

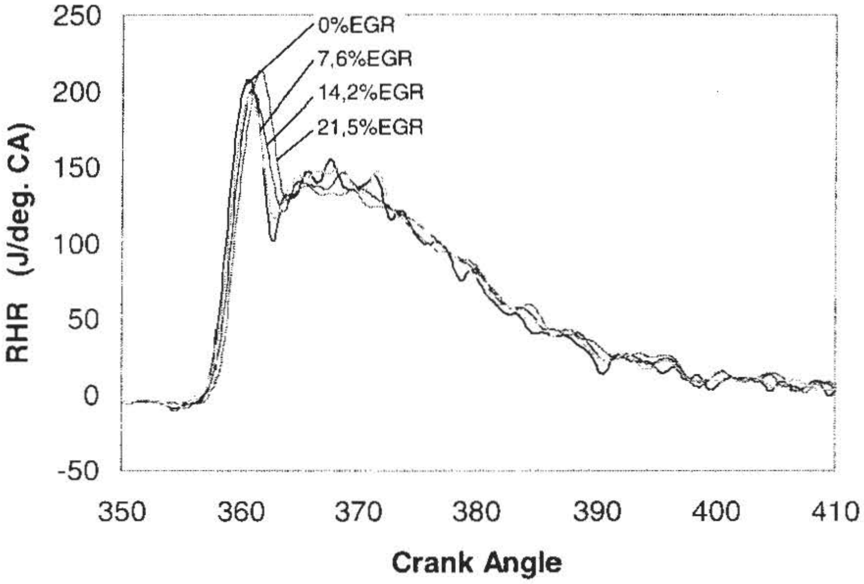

Fig. 7. Net-heat release curves with different EGR rates at 1600 rpm and p_e= 9 bar

curves shifted by ignition delay (Fig. 5) were observed. The combustion duration was approximately 60 ^{0}CA in all cases. The transition from premixed combustion into diffusion combustion was well defined for the original engine (0 % EGR). It became less explicit with increasing EGR rate. There were slight differences in the slope of the RHR curve in the first phase of premixed flame. The steepness of the curves decreased with EGR rate, which gave evidence of reduced reaction rates with lower oxygen concentrations. The peak RHR values were similar for all RHR curves and shifted according to differences in ignition delay. High oscillations during diffusion combustion did not allow detailed analysis of this part of RHR.

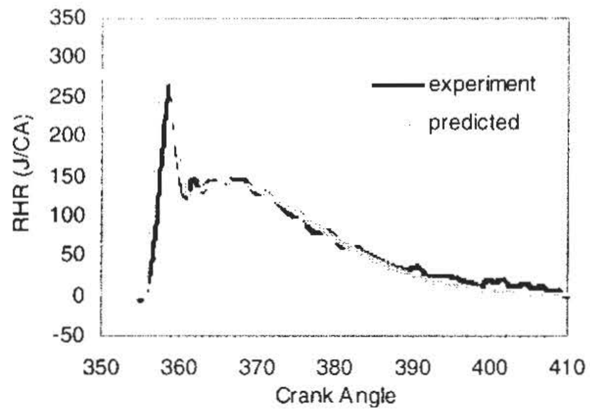

a) 1200 rpm

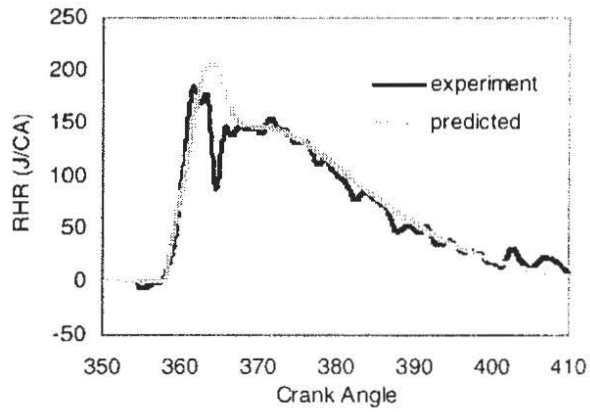

b) 2000 rpm

Fig. 8. Different RHR curves at p_e= 9 bar and 0 % EGR

Several empirical models can be used for RHR simulation. The most simple are one-zone models employing so called Viebe functions [9] to correlate RHR curve. Watson's model [9] was found almost perfect to simulate RHR of tested engine when no EGR was applied. The agreement between simulated and experimentally obtained RHR is very good as it can be seen from Fig. 8. The same model was applied, therefore, to simulate RHR with different EGR rates, and it was found fairly good when used with the corrected ignition delay equation (4). Fig. 9 shows how important is the correct prediction of ignition delay when RHR is simulated using Watson model. Ignition delay predicted by original model (Fig. 6) is too short. Consequently the predicted premixed burn is reduced as well, and, therefore, the intensity of premixed combustion is under predicted. On the other hand the intensity of diffusion combustion is over predicted. With the corrected ignition delay model the premixed burn is better predicted and both premixed and diffusion combustion rate agree fairly well with experimentally obtained results.

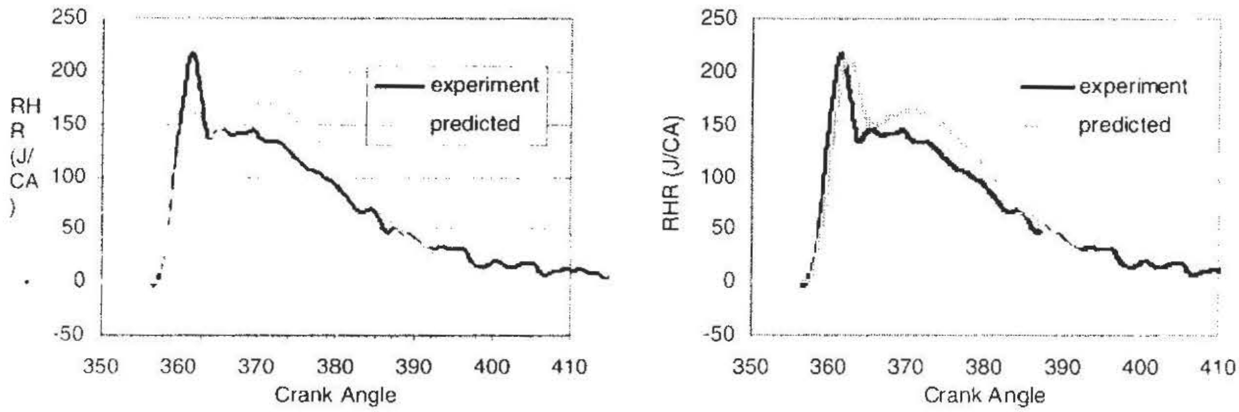

a) original ID model *b) corrected ID model*

Fig. 9. Different predicted RHR curves at 1600 rpm, p_e= 9 bar and 21 % EGR

4. Conclusions

The effect of EGR on the macro characteristics of diesel combustion was studied. In-cylinder pressure and injector needle lift traces were recorded and used to predict some basic macro characteristics of combustion. It may be concluded that the reduction of oxygen concentration within the fresh cylinder charge influences combustion and NOx reduction the most, ignition delay is increased with EGR and premixed combustion accelerates slower in the reduced oxygen atmosphere, and attains lower combustion rate peaks. A simple correction of ignition delay prediction model when used with EGR was found and the importance of correctly predicted ignition delay in RHR simulation was shown.

References

[1] Needham J.R., Doyle D.M., Nicol A.J., The low NOx truck engine, SAE Paper 910731

[2] Uchida N., Daisho Y., Saito T., Sugano H., Combined effects of EGR and supercharging on diesel combustion and emissions, SAE Paper 930601

[3] Heywood J.B., Internal combustion engine fundamentals, McGrawHill, New York. 1988

[4] Mattes P., Remmels W., Sudmanns H., Untersuchungen zur Abgasruecfuerung am Hochleistungs-dieselmotor, MTZ Motortechische Zeitschrift 60 (1994) 4, pp. 234 - 242

[5] Mitchell D.L., Pinson J.A., Litzinger T.A., The effect of simulated EGR via intake airdilution on combustion in an optically accesible DI diesel engine, SAE Paper 932798

[6] Zhao H., Hu J., Ladommatos N., In-cylinder studies of the effect of CO2 in exhaust recirculation on diesel combustion and emissions, Proc Instn Mech Engrs, Vol 214, Part D, D08499, ImechE 2000, pp. 405 - 419

[7] Ladommatos N., Balian R., Horrocks R., Cooper L., The effect of exhaust gas recirculation on combustion and NOx emissions in a high-speed direct-injection diesel engine, SAE Paper 960840
[8] Dimitriu D.G., Ziejewski M., Goettler H., A study of energy released during premixed combustion, SAE Paper 932478
[9] Dobovišek Ž., Predictive zero-dimensional single-zone models diesel combustion simulation models, Strojniški vestnik, ISSN 0039-2480, - 39 (1993), 5 – 9, pp. 137 - 160